ELSEVIER

Carbohydrate Research 308 (1998) 133–147

# Gelatinisation of starch: a combined SAXS/WAXS/DSC and SANS study

Paul J. Jenkins, Athene M. Donald *

*Cavendish Laboratory, Madingley Road, Cambridge CB3 0HE, UK*

Received 31 July 1997; accepted in revised form 21 March 1998

**Abstract**

Using a combination of techniques, small- and wide-angle X-ray scattering, differential scanning calorimetry and small-angle neutron scattering, it has been possible to follow the stages that occur during gelatinisation in excess water for a range of starches. It is found that water enters the amorphous growth rings first, and that this is where all the swelling is concentrated. The periodicity of the semicrystalline stack remained unchanged as long as the crystallites can still be identified. As the temperature is raised further through the gelatinisation endotherm, the crystallites become destabilised and the crystallisation index drops to zero, rather beyond the end of the endotherm revealed by DSC. 

*Keywords:* Starch; Gelatinisation; Neutron scattering; X-Ray scattering; Crystallinity; Growth ring

## 1. Introduction

When heated in the presence of water, starch undergoes an irreversible order–disorder transition termed gelatinisation. The granules are observed to swell, absorb water, lose crystallinity, and to leach amylose. Many techniques, including differential scanning calorimetry (DSC), X-ray scattering, light scattering, optical microscopy, thermomechanical analysis (TMA) and NMR spectroscopy have been employed to study these events in an attempt to understand the precise structural changes underlying gelatinisation. Based on these studies, various models have been proposed but, as yet, a universally accepted explanation of the gelatinisation process is still lacking [1].

The starch granule is known to be semicrystalline, and this gives rise to birefringence when viewed between crossed polars. As the starch granules gelatinise and their structure is disrupted, this birefringence is lost. Many studies have attempted to characterise the point at which all birefringence is lost for a sample studied under an optical microscope. This point is termed the birefringence end point temperature (BEPT). Whereas the loss of birefringence occurs over quite a large temperature range for the whole sample (a BEPT range of 56–64 °C has been measured for 12% starch (w/w) suspensions of wheat and potato starches heated at 1.5 °C/min [2]), individual granules are observed to lose birefringence over a much smaller range, generally less than 1 °C [3].

During the gelatinisation process, substantial swelling occurs. Concomitant with this, loss of crystallinity occurs as demonstrated by wide-angle

* Corresponding author.

0008-6215/98/$19.00 
*PII* S0008-6215(98)00079-2

X-ray scattering (WAXS) studies. Crystallinity loss has been quantitatively correlated with thermal events (as measured by DSC) in a detailed study by Liu et al. [4]. Assuming that a given decrease in crystallinity gives rise to a constant enthalpy change, a plot of the derivative of crystallinity with respect to temperature should mirror the DSC curve. This was observed to be qualitatively true for the samples studied in the earlier study [4]. However, since the samples used in the two experiments had undergone different thermal treatments, direct comparison between the curves was not possible.

A similar investigation was made by Cooke and Gidley [5] with the additional use of NMR to measure double helix content. They observed that crystalline and molecular order are lost concurrently during gelatinisation. Further work included measurements of birefringence loss [6], and it was demonstrated that birefringence loss started earlier and concluded earlier than molecular and crystalline order loss, as also found by Liu et al. [4]. However, it should be recognised that in these studies, measurements of order were made by post mortem study, and not in situ, raising the possibility of some uncertainties in the quantitative results.

In contrast to this, the use of synchrotron radiation permits real-time X-ray studies to be made during heating. The initial experiments carried out by Cameron and Donald [7–9] used small-angle X-ray scattering (SAXS) to study changes in electron density occurring when starch samples were held at a fixed temperature within the gelatinisation range. Electron density information was obtained by fitting the measured SAXS profile to a theoretical prediction for a model structure with variable electron densities. Regions representing crystalline lamellae, amorphous lamellae and amorphous background material (which is thought to correspond to the amorphous growth rings known to exist in the granule, probably due to diurnal fluctuations [10]) were included in the model. Results for wheat starch indicated that electron density changes take place first within the amorphous background region, suggesting that initial water absorption occurs within this. Subsequent changes in electron density were consistent with crystallite melting induced by water absorption into the amorphous lamellae.

More recent instrumental developments now permit both SAXS and WAXS data to be collected simultaneously while heating the sample through the gelatinisation range. A description of the method and preliminary results for wheat starch have already been presented [11]. The aim of the present paper is to extend the technique to a wide range of different types of starch and, coupled with small-angle neutron scattering (SANS) experiments, to explore the validity of the different models current in the literature to explain the gelatinisation process.

*Existing models for gelatinisation.*—Broadly speaking, there are currently four approaches in the literature (although there is something of a continuum of interpretation), which differ in various key features. The earliest model is that of Donovan [12]. In this model, the swelling of the amorphous regions of the granule is considered to 'strip' starch chains from the surface of crystallites, thereby disrupting crystalline order. This swelling-driven process generates the DSC endotherm (referred to as G). In conditions of limiting water (usually defined as conditions in which a second endotherm is seen in DSC measurements), there is insufficient water present for all the crystallites to be disrupted in this manner. Crystallites located in areas of locally high concentrations of water undergo 'stripping', giving rise to the G endotherm; those remaining after the conclusion of this process undergo 'melting' at higher temperatures, giving rise to the M1 endotherm. If the water content is reduced still further, none of the crystallites undergo the 'stripping' process, and only the M1 melting endotherm is observed. Since crystallite 'stripping' could be assumed to result in unfolding and hydration of helices, this model is consistent with the observation of concurrent loss of crystalline and molecular order. Certain ambiguities still remain, however, notably in the location of the amorphous regions whose swelling precipitates gelatinisation.

Blanshard [1] subsequently suggested a reinterpretation of the Donovan gelatinisation model. He postulated that the G endotherm was a consequence of chain mobilisation in the amorphous regions. In excess water, this led to the gross swelling and crystallite disruption proposed by Donovan. However for a limiting water system swelling of the amorphous regions had little effect on the crystallites, which therefore melted out at higher temperatures generating the M1 endotherm. The more recent studies by WAXS on the disruption of granular crystallinity have contradicted Blanshard's

observation and suggested instead that crystallinity is lost throughout both G and M1 endotherms [4,13]. However, these experiments are open to the accusation that since measurements are not made in situ, structural modification may occur when extracting the partially gelatinised samples. The results could therefore still be considered somewhat ambiguous.

Based on the observation that individual granules are observed to lose birefringence over a much smaller range than the total population, Evans and Haisman [14] proposed a highly co-operative 'positive feedback' mechanism for the gelatinisation of a single granule. For granules in excess water, they postulated that the melting of the least stable crystallite within a granule removed some of the swelling constraints, allowing the granule to absorb more external water. This had the effect of lowering the melting point of the remaining crystallites, facilitating the absorption of more water and the melting of more crystallites. Thus, each granule melts over a very small temperature range.

This mechanism can also be used to explain the effect of reducing the water content. In conditions of limiting water, granules containing the least stable crystallites gelatinise by the mechanism outlined above. However, there will come a point at which all the free water has been absorbed. After this point, there is no more co-operativity between the melting of different crystallites; consequently the remaining crystallites melt at higher temperatures. It is postulated that the melting of these remaining crystallites generates the M1 endotherm. It should be noted that this model does not attribute any significance to the amorphous regions in the starch granule. It is difficult to reconcile this model with the crystallinity, molecular order and birefringence studies of Gidley and Cooke [5,6]. They measured birefringence loss to occur before the onset of appreciable crystallite melting. Assuming birefringence loss to indicate the onset of gelatinisation, this suggests that crystallite melting does not initiate gelatinisation.

Finally, it has been suggested by Biliaderis that the two endotherm DSC behaviour in limiting water is a consequence of partial melting followed by recrystallisation and final melting [15]. Evidence for this came from the effect of heating rate, which caused the G and M1 transitions to merge. It was suggested that, at the higher heating rate, insufficient time was available for recrystallisation. In excess water, it is suggested that gelatinisation is precipitated by the occurrence of a glass transition within the bulk amorphous phase whereupon melting and recrystallisation processes occur simultaneously. However, as the water content is reduced the difference between glass transition and melting temperature increases, thus separating the melting and recrystallisation transitions so that they can be independently resolved by DSC. However, more recent studies have suggested that a glass transition is unlikely to occur immediately prior to gelatinisation [16,17]. Furthermore, the effect of heating rate on the two endotherms can also be explained in terms of changes in the resolution of the DSC instrument [18]. It should also be noted that recrystallisation was not observed in X-ray studies of partially gelatinised starch prepared by extracting samples during gelatinisation in limiting water [4,13].

This brief summary of the state of existing gelatinisation models indicates both that there is disagreement in the literature, and that the situation is still unresolved. The model with least experimental evidence running counter to it is that due to Donovan. In this paper our results will allow us to make refinements to this model to build up a clearer picture of the processes involved in gelatinisation.

## 2. Experimental

*Materials*.—Wheat starch was a gift from the Institute of Food Research, Norwich; potato starch was a gift from Dalgety Food Technology Centre, Cambridge; maize starch and rice starch were obtained from Sigma Chemicals Ltd; tapioca was a gift from National Starch and Chemical, Manchester; and wild type pea was a gift from Dr A. Smith, John Innes Institute, Norwich. Of these wheat, maize, waxy maize, rice and tapioca have A-type crystalline structures, potato and amylomaize have B-type crystalline structures and wild type pea has a C-type crystalline structure.

For all samples, the sample moisture content was established by recording the weight loss after storage in a vacuum oven at 70 °C for 6 h. These water contents are detailed in Table 1. A knowledge of the initial moisture content for the samples enabled mixing of samples with water to obtain the same water content on a dry weight basis. All samples were studied at a starch concentration of 40% (w/w), except for those used in the SANS

Table 1
Moisture contents of air-dry starch samples

| Starch | Moisture content (%) |
|---|---|
| Wheat | 11.5 |
| Potato | 14.4 |
| Maize | 9.9 |
| Rice | 10.6 |
| Tapioca | 13.4 |
| Wild type pea | 12.7 |
| Waxy maize | 12.6 |
| Amylomaize | 12.6 |

experiments when, for practical reasons, a concentration of 45% (w/w) was used.

*Experimental set-up for in situ simultaneous SAXS, WAXS and DSC.*—X-ray experiments were carried out on station 8.2 at the Daresbury Laboratory. The experimental arrangement has been described previously [11,19]. Heating was carried out using a heat flux DSC. This was a modified Linkam THM microscope hot stage. The design and construction of this DSC is described in more detail elsewhere [20]. Starch slurries in water were sealed in modified Du Pont DSC pans. Two gas-filled proportional wire chambers were used to collect the diffraction patterns. X-rays scattered through wide angles (from $\sim 8°$–$90°$ $2\theta$) are detected by an Inel detector. Simultaneously, X-rays scattered through smaller angles ($< \sim 6°$ $2\theta$) were detected by a quadrant detector. The low divergence, high intensity beam of radiation with approximately the wavelength of $CuK_\alpha$ ($\lambda = 1.5$ Å) was collimated with slits and focused at a point half way between the two detectors.

For each sample, a measurement of the X-ray scattering at room temperature was taken first. Then the DSC was programmed to heat from room temperature up to 120 °C at a predetermined rate. The two heating rates used in this study were 2 and 5 °C/min. The collection of X-ray diffraction patterns was triggered by a pulse from the DSC as the heating run began. During the heating run, simultaneous in situ measurements of SAXS and WAXS patterns were made. The collection time for a single pattern was typically 12 s.

*SAXS analysis.*—Small angle scattering profiles were corrected as described previously [7]. The data were divided by the detector response, normalised with respect to the intensity of the beam exiting the sample, and the background scattering and constant liquid scattering term were subtracted. The channel numbers of the detector were calibrated against wave number using wet rat tail collagen. Data collected during different sessions at Daresbury have all been normalised to the same arbitrary intensity scale. This arbitrary scale is chosen such that the electron density difference between crystalline and amorphous lamellae for 40% (w/w) wheat starch at room temperature is equal to 1. Information concerning the changes occurring in long-range order during gelatinisation was obtained using the method described previously [9]. Each SAXS profile was independently fitted by a model scattering function, and structural parameters read off when the best correlation was obtained between predicted and observed scattering.

*WAXS analysis.*—Data collected on the Inel detector was normalised to the intensity of the direct beam (measured by an independent ion chamber to correct for fluctuation in incident X-ray flux) and divided by the total integrated intensity over the region of interest. This second correction normalises the data to equal scattering mass [21]. The region of interest was chosen to include most of the major diffraction peaks. Corrections for cosmic and radioactive background count and for detector inefficiency were found to have little effect on the data and were therefore ignored.

Values of crystallinity index, based on the method of Wakelin [22], were obtained from the gradient of a least squares fitted line to a plot of $(I_u - I_a)_{2\theta}$ versus $(I_c - I_a)_{2\theta}$ where $I_u$, $I_a$ and $I_c$ are the scattered intensities at a given value of $2\theta$ for the data set, and for the amorphous and crystalline reference samples, respectively. These reference samples were chosen as the last (fully gelatinised) and first (ungelatinised) data points as a function of temperature, respectively. It should be noted that this method takes into account all reflections associated with order, including the interhelix peak. This factor will become important in the discussion below.

*DSC.*—The data obtained from the Daresbury heat flux DSC is noisy, but can be used as a temperature calibration. For the small endothermic transitions accompanying starch gelatinisation, it is difficult to use the in situ DSC data for accurate measurement of endotherm start, onset, peak and conclusion temperatures. Accurate measurements of these temperatures were instead made on a Perkin-Elmer DSC-7 equipped with an Intracooler II. Small (15–20 mg) samples of starch slurry of the same starch:water ratio used in the X-ray experiments were hermetically sealed inside 50 μL

aluminium pans, and heated at the same temperature rate and over the same temperature range as for the X-ray measurements. From the DSC trace, measurements were made of the start ($T_s$), onset ($T_o$), peak ($T_p$) and conclusion ($T_c$) temperatures. The start and conclusion temperatures are defined as the point at which the DSC trace first starts and finally ceases to deviate from a flat baseline, respectively. The onset temperature is defined as the point at which a straight line drawn down the leading edge of the DSC endotherm intersects the baseline. The peak temperature is defined as the point of maximum endothermic heat flow relative to the baseline. Measurements of these values are based on the mean of three runs, with associated uncertainties of less than 1 °C.

*SANS*.—Experiments were carried out only on waxy maize on the LOQ beamline at the Rutherford Appleton Laboratory. The application of SANS to the study of waxy maize starch at room temperature has already been described [23], and only an outline of the experimental technique will be given here. The basic principles of SANS and SAXS are similar, but the ability to change the contrast causing the scattering by changing the proportion of $D_2O$ in normal water introduces a new variable into the problem. By using eight different contrasts (100, 90, 80, 60, 40, 20, 10 and 0% $H_2O$ on a molar basis), it becomes possible to extract not only the equivalent parameters to those obtained from SAXS, but also the proportion of water in each of the three types of region within the granule. It is this new type of information which is so useful in helping to interpret the gelatinisation process. However, it should be recognized that due to the number of stages in fitting the data, which is itself inherently noisy, great precision in the final water contents cannot be expected.

Samples of water with the required molar ratio of $H_2O$ to $D_2O$, $x$, were prepared first, and then added to vacuum dried waxy maize starch to form 45% (w/w) starch slurries. Waxy maize starch was chosen for these studies because the SAXS studies have shown it exhibits an intense Bragg peak which can be particularly accurately fitted [24]. Since the signal:noise ratio is inherently worse in these SANS experiments than for SAXS, it seemed prudent to inititate studies on a strong scatterer. To ensure complete exchange, the samples were left to stand for 24 h, the starch filtered off, dried in a vacuum oven, then re-slurried in the same concentration with more water of the same molar ratio of $H_2O$ to $D_2O$. A standing time of 24 h was chosen with reference to infrared studies that have shown that hydrogen–deuterium exchange in starch reaches an equilibrium after 24 h [25]. The slurries were mixed in 1 mm path length quartz cells obtained from Helma (part number 6100, blue). Quartz cells were used since they are transparent to neutron beams. The neutrons scattered from the sample cell were detected by a $^3$He detector situated 4.4 m distant from the sample. The neutron beam was collimated to a size of 8 mm diameter at the sample. The analysis of the scattering was as described previously [23].

## 3. Results

Typical DSC profiles for 40% (w/w) starch mixtures in water during gelatinisation at a heating rate of 5 °C/min are shown in Fig. 1. For each starch sample at least three DSC traces were recorded. The gelatinisation parameters obtained from these traces are detailed in Table 2.

Samples of wheat, potato, maize, rice, tapioca and wild type pea starch in water (40% (w/w)) were heated in situ in the X-ray beam using the Daresbury DSC. The heating rate was 5 °C/min. Simultaneously WAXS profiles were collected. The crystallinity index was calculated for each sample independently as a function of temperature. These plots are shown in Fig. 2. Qualitative studies on the WAXS profiles for these starches suggested that for no sample was there a significant shift in any of the wide-angle diffraction peaks during gelatinisation.

Simultaneously with the collection of WAXS data, SAXS profiles were also collected. These SAXS profiles were analysed as described previously [9,11].

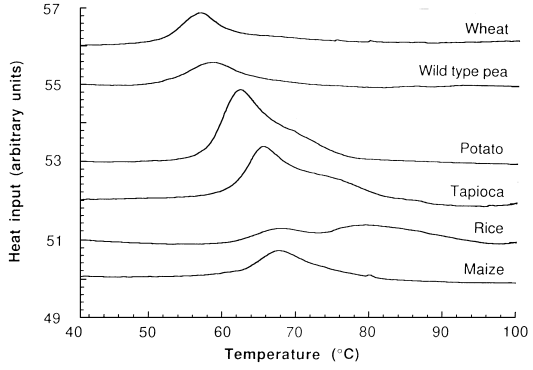


Fig. 1. Effect of botanical source on DSC gelatinisation characteristics. DSC traces for 40% (w/w) starch mixtures in water, heated at 5 °C/min

Table 2
Start ($T_s$), onset ($T_o$), peak ($T_p$) and conclusion ($T_c$) temperatures and enthalpies ($\Delta H$) for the gelatinisation endotherm for different botanical sources of starch. Enthalpy values are expressed in J/g of dry starch. Measurements were made on a Perkin Elmer DSC heating at 5 °C/min

| Starch sample | $T_s$ (°C) | $T_o$ (°C) | $T_p$ (°C) | $T_c$ (°C) | $\Delta H$ (J/g) |
|---|---|---|---|---|---|
| Wheat | 45.2 ± 0.4 | 51.2 ± 0.1 | 56.0 ± 0.2 | 76 ± 1 | 9 ± 1 |
| Potato | 52.9 ± 0.6 | 57.2 ± 0.2 | 61.4 ± 0.3 | 80.3 ± 0.4 | 17.4 ± 0.4 |
| Maize | 58 ± 1 | 62.3 ± 0.3 | 67.7 ± 0.2 | 84 ± 1 | 14 ± 2 |
| Rice | 56 ± 2 | 62.0 ± 0.2 | 67.4 ± 0.1 | 97.5 ± 0.4 | 11 ± 1 |
| Tapioca | 54 ± 1 | 60.9 ± 0.2 | 65.3 ± 0.2 | 88 ± 2 | 20 ± 1 |
| Wild type pea | 45 ± 2 | 51.9 ± 0.8 | 58.3 ± 0.2 | 83 ± 1 | 6.5 ± 0.3 |

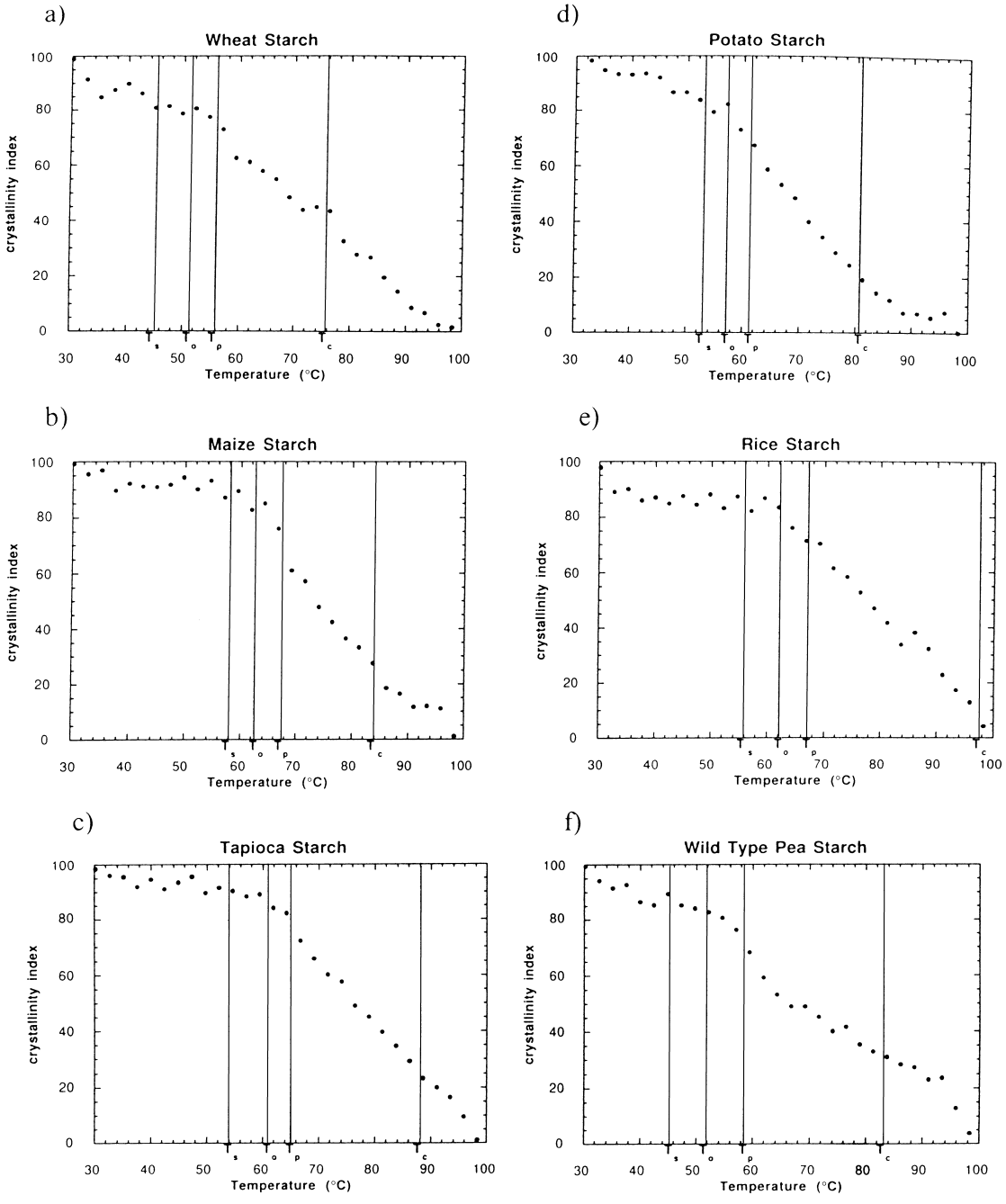


Fig. 2. Variation in crystallinity index with temperature during the gelatinisation of 40% (w/w) starch samples in water

Structural information was obtained by fitting each individual SAXS data set to the model function described previously [7]. An initial fit for the starch sample at room temperature allowed variation in all the six parameters of the model: the number of lamellae in the stack ($N$); the average repeat distance between crystalline lamellae ($d$); the fraction of this repeat distance that is crystalline ($\phi$); a parameter defining the distribution of lamellar sizes ($\beta$), and two scattering density differences, between crystalline and amorphous lamellae ($\Delta\rho$) and between amorphous lamellae and amorphous background ($\Delta\rho_u$). However, for fits to the subsequent data sets for all the starch samples, it was found necessary to vary only two of these six available parameters: the two electron density differences, $\Delta\rho$ and $\Delta\rho_u$. Figs. 3 and 4 detail the variation in these electron density differences with temperature. Initial room temperature values for the parameters $\beta$, $N$, $d$ and $\phi$ have been given previously [24,26], and remained the same during gelatinisation.

*SANS on waxy maize*.—From scattering profiles using the different contrasts, it was possible to obtain the six parameters analagous to those obtained for SAXS. To fit all the waxy maize gelatinisation SANS profiles, it was found necessary to vary only the values of the parameters $\Delta\rho$ and $\Delta\rho_u$, equivalent to the situation for SAXS. The other four parameters remained fixed at the values given in Table 3, obtained from the fit at room temperature.

The variation in the values of $\Delta\rho$ and $\Delta\rho_u$ with temperature during gelatinisation of 45% waxy maize starch in 10% $H_2O$, 90% $D_2O$ are detailed in Fig. 5a and b. Combining these results with those for the five other water and deuterium oxide contents studied, and applying the analysis described in the earlier paper for waxy maize at room temperature [23], we obtained values for the water content in the three regions of the granule ($f_b, f_a, f_c$ for the amorphous background, amorphous lamellae and crystalline lamellae, respectively), and $\rho_b$, $\rho_a$, and $\rho_c$, the starch molecular density in the three regions, as a function of temperature. These results are displayed in Figs 6 and 7. Using these values of $f_b, f_a, f_c$, $\rho_c$, $\rho_a$, and $\rho_b$, it was possible to calculate scattering length densities for each of the three regions within the starch granule [23]. For 45% waxy maize starch in 90% $H_2O$ and 10% $D_2O$ Fig. 8a and 8b record how $\bar{b}_b$, $\bar{b}_a$, and $\bar{b}_c$ vary as a function of temperature during gelatinisation.

## 4. Discussion

For all the samples, it can be seen from Fig. 2 that there is an initial gradual drop in the crystallinity index from room temperature until somewhere between the onset and the peak temperature of the DSC endotherm. After this point, the rate of crystallinity loss increases. At the conclusion temperature for the DSC endotherm, there is still some residual crystallinity. These plots indicate that for all the starches covered in this study, most (but not all) crystallinity loss occurs for temperatures within the gelatinisation endotherm. It is important, however, to emphasise the observation that changes in crystallinity index occur both prior to the start and after the conclusion temperature of the measured endotherm. This observation is made without exception for the range of different starches covered here. It would seem that DSC measurements, which are widely used to study starch gelatinisation, do not tell the whole story. Since the range of crystallinity loss exceeds the range of the DSC endotherm, we may conclude that in some senses the gelatinisation process itself occurs over a wider temperature range.

That the crystallinity index remains substantial beyond the end of the gelatinisation endotherm (whereas this is not the case for the measures of order determined by SAXS) requires some discussion. One approach to resolving this apparent paradox is to consider what the crystallinity index is actually measuring: it uses all reflections and therefore includes the order associated within double helices, as well as the full three-dimensional crystal structure. However, this long-range crystallinity could be lost before the double helices themselves dissociate. This interpretation of a decoupling of long- and short-range order is supported by additional experiments on potato starch [27], which indicate that the peak associated with interhelix scattering is still detectable (albeit much reduced in magnitude) at temperatures as high as 85 °C, i.e. beyond the apparent end of the DSC endotherm ($T_c$ in Fig. 2d corresponds to around 80 °C). In this case, the question of why the enthalpy associated with subsequent loss of helicity is not revealed in the DSC experiments remains unclear. The study of loss of molecular versus crystalline order as a function of temperature [5] suggests that there should be substantial enthalpy associated with helix disassociation, although the conclusions are based on post mortem analysis

which could conceivably explain the apparent discrepancy. Furthermore, it is possible that since the number of helices remaining at higher temperatures may be comparatively small, their disordering could be lost in the baseline of a DSC experiment. Further experiments to explore the nature of the high temperature structural loss will be required to resolve this issue.

The shape of the crystallinity index curves are broadly consistent with that obtained for maize starch in an earlier study [4]. Starch, gelatinised in excess water, loses crystallinity over a wide range

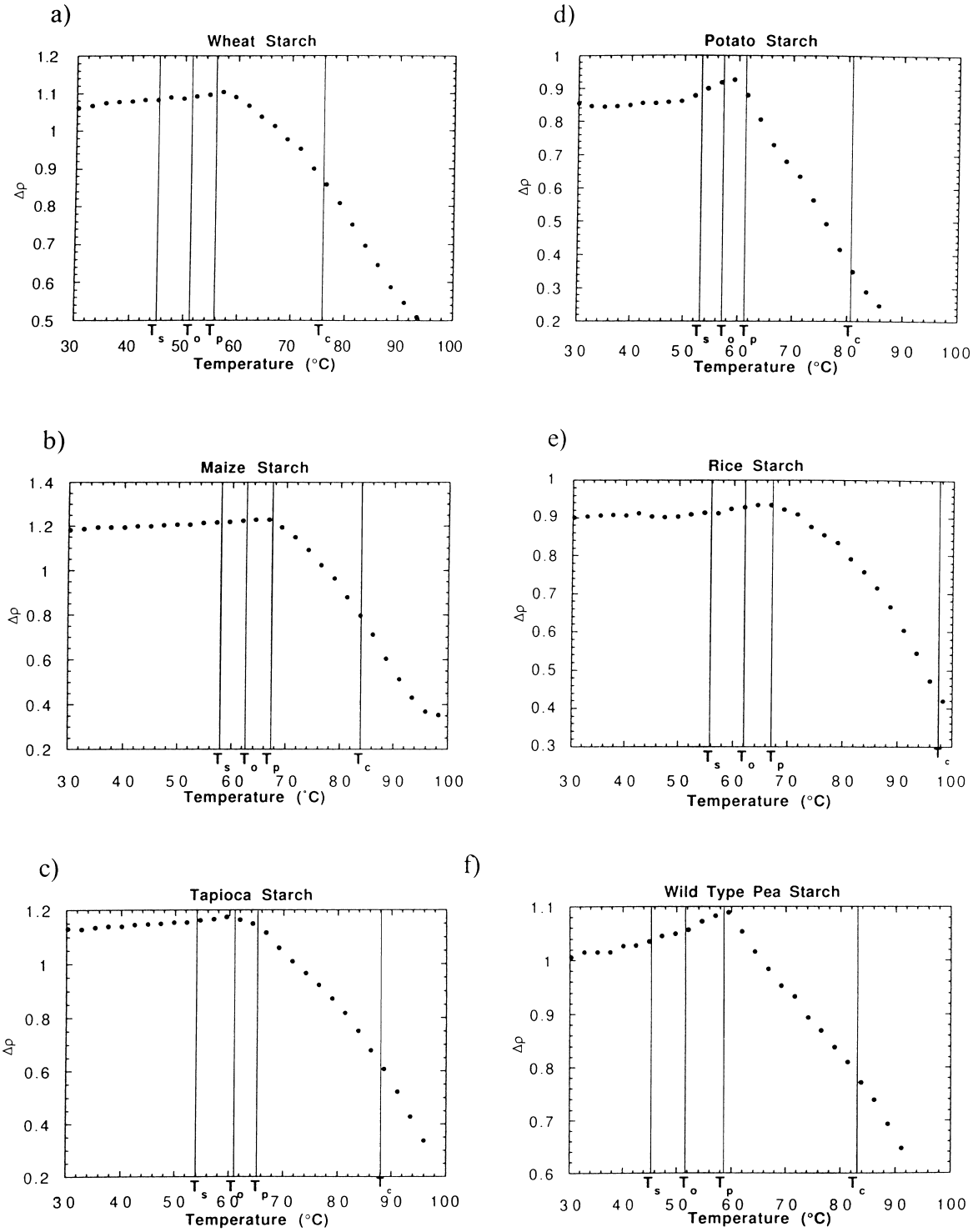


Fig. 3. Variation in $\Delta\rho$ (the difference in electron density between the crystalline lamellae and the amorphous lamellae) with temperature during the gelatinisation of 40% (w/w) starch samples in water

of temperatures. In ref. [4] the measurements of crystallinity index were not made in situ, but on pre-prepared partly gelatinised samples. As a result, direct correlation with DSC data was not possible. However crystallinity index loss was accurately correlated with birefringence loss. It was observed that birefringence loss occurred over a much narrower range than crystallinity loss, and was completed well before all crystallinity had been lost. This observation is not unexpected since birefringence requires structural ordering over a long range, whereas crystallinity can exist over a much shorter structural range. Consequently, the sample will lose birefringence when any part of the long-range

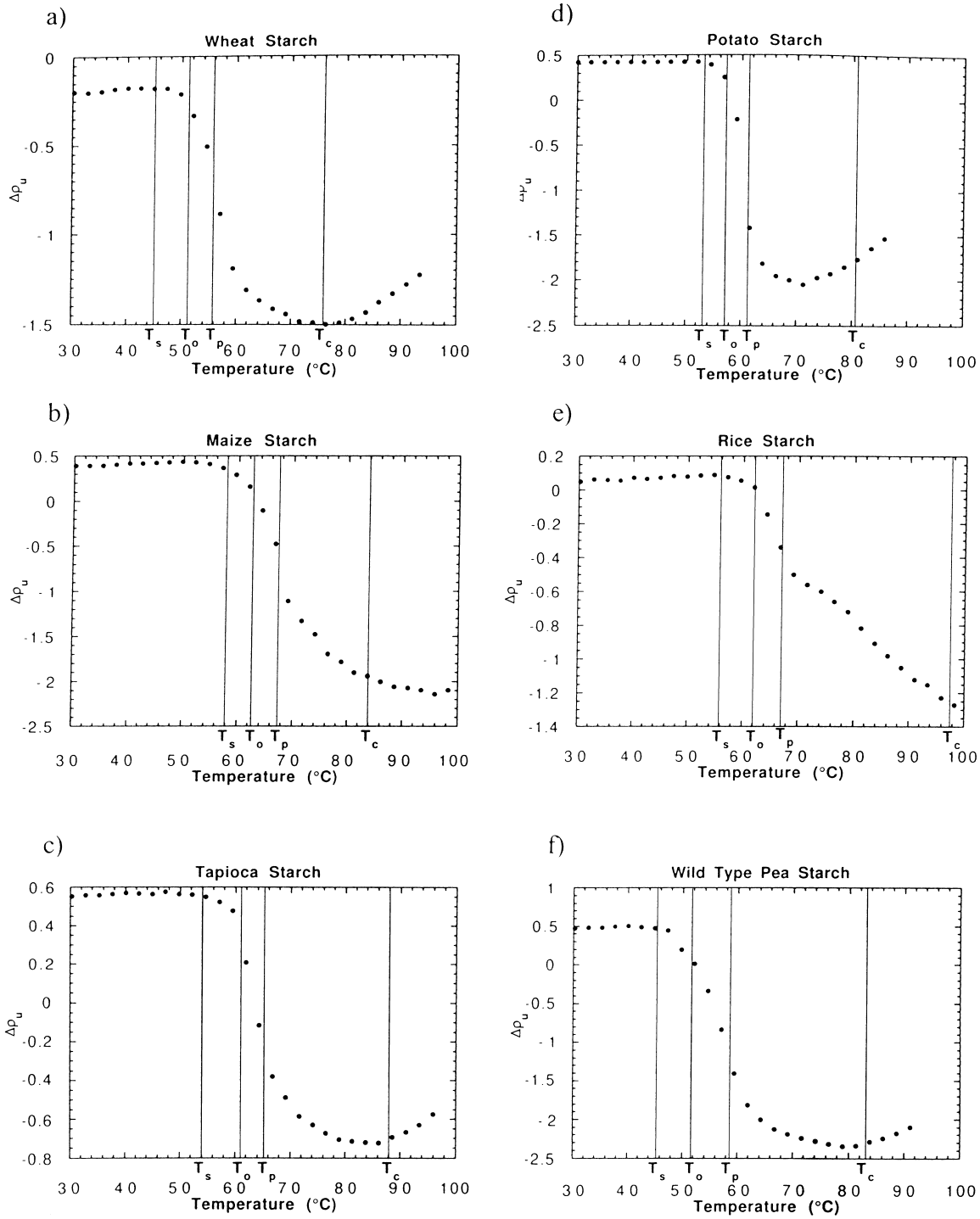


Fig. 4. Variation in $\Delta\rho_u$ (the difference in electron density between the amorphous background and the amorphous lamellae) with temperature during the gelatinisation of 40% (w/w) starch samples in water

order is disrupted, whilst crystallinity loss involves the disruption of smaller groupings of double helices. Our study supports these findings.

Considering the case of potato starch specifically, we find the crystallinity is principally lost between 57 and 90 °C. For potato starch in excess water heated at 7 °C/min, Leszczyñski [28] recorded birefringence loss in situ in the range 58–75 °C. These results suggest that birefringence measurements, which are widely used to monitor polymer melting, provide only an approximation of the final melting point of starch polysaccharides.

In agreement with the WAXS data, the SAXS information suggests striking similarities in the gelatinisation behaviour of the different starches. For all starch samples, having obtained an accurate fit to the room temperature SAXS profile, it was possible to fit all subsequent higher temperature SAXS profiles by varying only the two electron density differences. Changes in $\Delta\rho$ and $\Delta\rho_u$

Table 3
Parameters derived from SANS for waxy maize at room temperature [23]

| $d$ | $N$ | $\phi$ | $\beta$ | $\Delta\rho$ | $\Delta\rho_u$ |
|---|---|---|---|---|---|
| 89 | 24 | 0.69 | 0.35 | 2.42 | −0.20 |

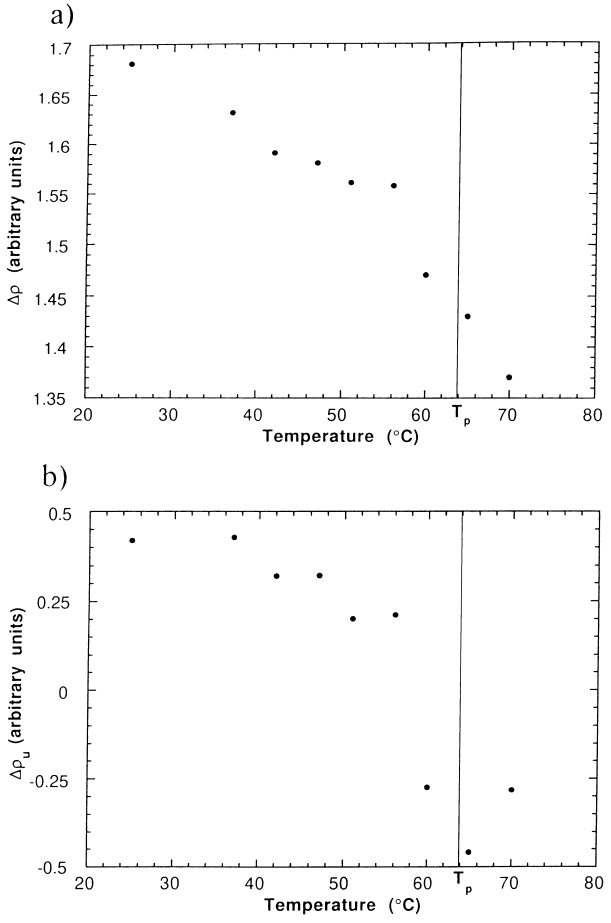


Fig. 5. Variation in (a) $\Delta\rho$ and (b) $\Delta\rho_u$ during gelatinisation for 45% waxy maize starch in 10% $H_2O$, 90% $D_2O$. Results obtained from analysis of SANS data

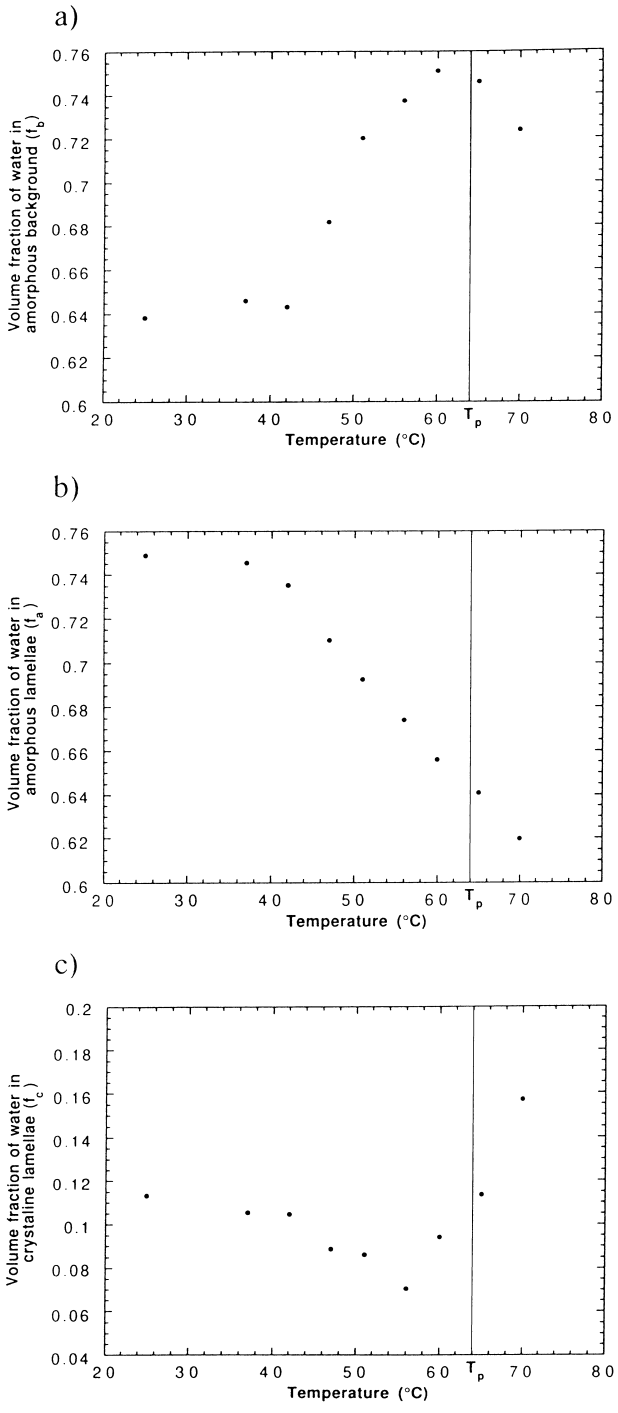


Fig. 6. Variation in water content (volume fraction) of (a) the amorphous background region, (b) the amorphous lamellae, (c) the crystalline lamellae with temperature during gelatinisation of 45% waxy maize starch

for the six starch samples are detailed in Figs 3 and 4, respectively. Once again, we observe a consistent behaviour across all starch species. There is an initial gentle rise in $\Delta\rho$, until a point, in between the onset and the peak temperature of the DSC endotherm. After this point the value of $\Delta\rho$ starts to fall. This fall in value continues beyond the conclusion temperature of the DSC endotherm. The initial rise in $\Delta\rho$ must be due to a drop in the value of $\rho_a$ (since it is not likely that $\rho_c$ rises), possibly associated with a small tangential expansion of the amorphous lamellae. The subsequent drop in $\Delta\rho$ is associated with a fall in the value of $\rho_c$ as the crystallinity within the crystalline lamellae is disrupted.

With regard to $\Delta\rho_u$, for all the starch samples, the first change occurred around the start temperature of the DSC endotherm. At this point, the value of $\Delta\rho_u$ dropped rapidly. With the exception of rice starch, this rapid drop has finished either just before or around the conclusion temperature of the DSC endotherm. This drop in the value of $\Delta\rho_u$ must be attributed to a fall in the value of $\rho_u$ for the background, as has previously been discussed for wheat starch [8]. This fall is itself associated with the absorption of water into and the resultant expansion of the background region.

Since from the SAXS data only the electron density differences within the model were found to vary during gelatinisation, all other structural parameters remain fixed at their pre-gelatinisation values. It is significant that the average repeat distance between crystalline lamellae remains invariant. This invariance indicates that the semicrystalline lamellar stack, representing the semicrystalline growth ring, does not itself expand radially during gelatinisation. Since the granule itself is known to exhibit quite pronounced radial expansion, we may conclude that this expansion is taking place solely within the amorphous background material, representing the amorphous growth ring. The lack of radial swelling observed for the semicrystalline growth ring is not entirely surprising. It is believed that amylopectin molecules within the semicrystalline growth ring adopt a cluster structure. This structure is essentially constructed from two types of amylopectin chain, short A chains forming the clusters, and longer B chains to connect the clusters. Any radial expansion would involve breaking many of these B chains, and is therefore unlikely. This conclusion is entirely consistent with the finding, discussed elsewhere [29], that the helical pitch does not change significantly during gelatinisation. If the crystalline lamellae within the semicrystalline

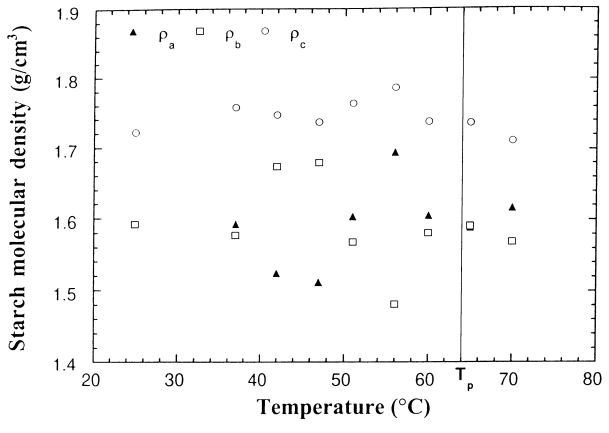


Fig. 7. Variation in starch molecular density within the crystalline lamellae ($\rho_c$), amorphous lamellae ($\rho_a$) and amorphous background ($\rho_b$) with temperature during gelatinisation of 45% waxy maize starch

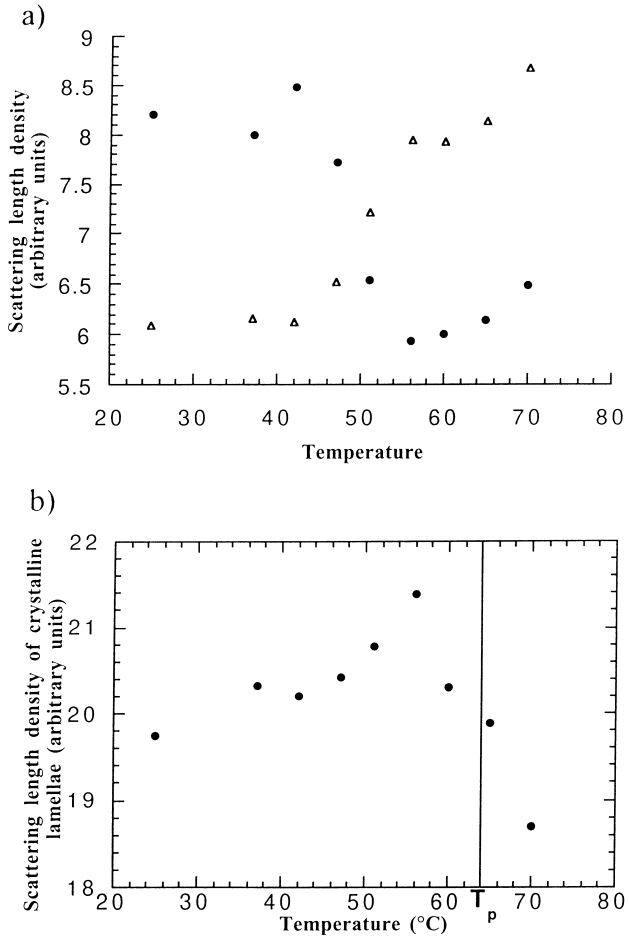


Fig. 8. Variation in scattering length density of (a) amorphous background region ($\bar{b}_b$) (●), and amorphous lamellae ($\bar{b}_a$) (△), and (b) crystalline lamellae ($\bar{b}_c$) in arbitrary units, as a function of temperature during gelatinisation of 45% waxy maize in 90% $H_2O$ and 10% $D_2O$

growth ring were expanding radially, we might expect to detect an increase in helical pitch.

These changes can be rationalised as follows. In excess (or close to excess) water, the first stage of gelatinisation is the uptake of water by, and rapid expansion of, the amorphous background region. Since this region is coupled to the semicrystalline lamellar stack, this swelling exerts a strong destabilising effect on the crystallites contained within the crystalline lamellae. As these crystallites are disrupted, so crystallinity is lost and the electron density of the crystalline lamellae falls. Since this behaviour is observed without exception for the six species of starch covered in this study, it would seem to represent a general gelatinisation mechanism for all starch granules in excess water. Further understanding can be gained from the SANS data to be discussed below.

For rice starch, the value of $\Delta\rho_u$ is still falling at 100°C. A clue as to the reason for this behaviour may lie in the DSC characteristics of rice starch at this water content. As shown in Fig. 1, rice starch is atypical of the starches studied in that it exhibits a clear second endotherm (defined as the M1 endotherm) at a temperature higher than that of the gelatinisation (G) endotherm even at a concentration of starch of 40%. This behaviour is generally associated with gelatinisation in limiting water, and it therefore appears that at this concentration rice starch is not in excess water conditions.

Before turning to the SANS data, it is worthwhile drawing the interpretation of these results together. Qualitatively, all six species behave similarly with regard to the SAXS/WAXS results as correlated with the DSC: the shapes of the curves seen in Figs 2–4 are broadly speaking the same. This finding suggests that the mechanism of gelatinisation is the same regardless of species. Nevertheless the details vary, both in the absolute values of the different parameters, and the temperatures at which changes occur. These variations no doubt reflect the impact both of the chemical nature of the amylopectin and amylose molecules (e.g. branch length, overall molecular weight, etc.) as well as the supramolecular structure, such as the percentage of the semicrystalline stack which is crystalline. That the temperature range of gelatinisation varies between species is well known from many previous DSC studies, but new information is provided by SAXS/WAXS which is an additional factor which needs to be taken into account as our understanding of the gelatinisation mechanism is refined.

Turning now to the SANS data, it is equally possible to fit all SANS profiles taken (for the waxy maize samples) during gelatinisation with the model scattering function, whilst varying only two of the six available parameters. The parameters that vary are the two scattering length density differences $\Delta\rho$ and $\Delta\rho_u$ (analagous to the electron density differences from SAXS). This corroborates the conclusion that the structural dimensions of the crystalline lamellae do not change during the gelatinisation process. This fact indicates that all the granule swelling observed during gelatinisation takes place within the amorphous growth ring.

The changes in $\Delta\rho$ during gelatinisation of 45% waxy maize in 10% water and 90% deuterium oxide, obtained from analysis of SANS profiles are detailed in Fig. 5a. Fig. 9 shows the same changes for 45% waxy maize starch in 100% $H_2O$ studied by SAXS. Both plots show a rapid drop in $\Delta\rho$ occurring just prior to the peak of the DSC endotherm. As discussed above, this is postulated to be due to a drop in the scattering density of the

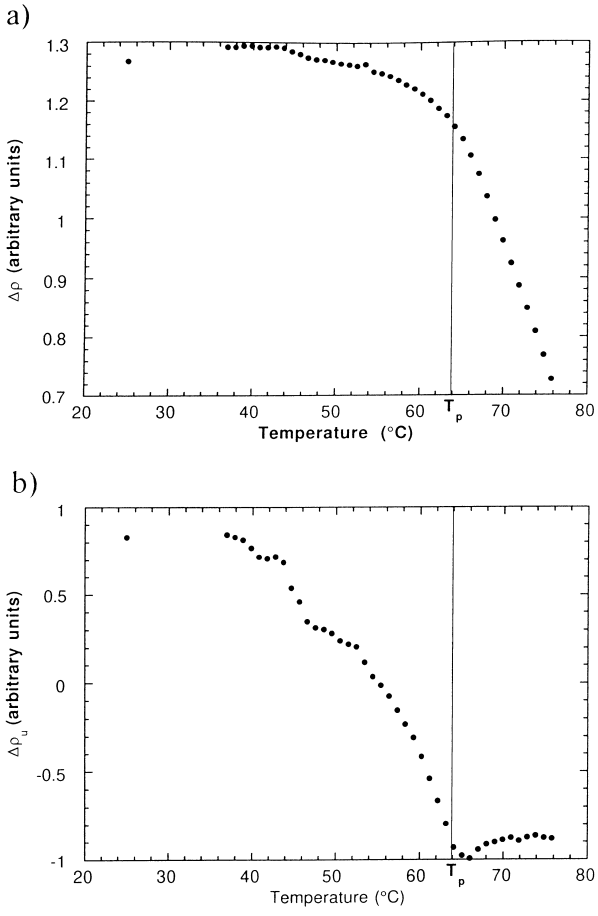


Fig. 9. Variation in (a) $\Delta\rho$ and (b) $\Delta\rho_u$ during gelatinisation for 45% waxy maize starch in $H_2O$ based on SAXS analysis

crystalline lamellae, both because of the disruption of crystalline structure within this region, and increased water penetration into this region.

The changes in $\Delta\rho_u$ during gelatinisation of 45% waxy maize in 10% water and 90% deuterium oxide, obtained from analysis of SANS profiles and which can be compared with Fig. 9b for the SAXS case (100% $H_2O$), are detailed in Fig. 5b. Once again, we observe a close similarity between these two plots. There is little change in scattering density before about 40 °C, then an increase in the magnitude of $\Delta\rho_u$ up to the peak of the DSC endotherm, and finally a constant value at temperatures greater than $T_p$, the peak of the gelatinisation endotherm. The interpretation of these effects is the same as for SAXS.

Using the neutron analysis technique described previously [23] we are, however, no longer restricted to simply measuring changes in scattering density differences. Instead, we are able to measure the changes in scattering density itself within each of the three intragranular regions independently. Fig. 8a–c show the changes in scattering density within the amorphous background, amorphous lamellae and crystalline lamellae during gelatinisation of a 45% waxy maize sample. The scattering length densities of amorphous lamellae, crystalline lamellae and amorphous background regions ($\bar{b}_a$, $\bar{b}_c$ and $\bar{b}_a$, respectively) remain constant at low temperatures. At around 45 °C $\bar{b}_a$ and $\bar{b}_c$ start to rise, whilst $\bar{b}_b$ starts to drop; $\bar{b}_a$ continues to increase in value throughout the gelatinisation process; $\bar{b}_c$ rises to a maximum at around 56 °C, before dropping off sharply; $\bar{b}_b$ drops to a minimum, constant value at around 56 °C.

With these results, we can now explain the changes observed in the values of $\Delta\rho$ and $\Delta\rho_u$. As suggested earlier, this reduction in the value of $\Delta\rho$ is due to a reduction in the scattering density of the crystalline lamellae; but this is only part of the story. The change is also due to an increase in the scattering density of the amorphous lamellae. This was not anticipated. With regard to $\Delta\rho_u$, the postulate based on the SAXS data that the increase in magnitude and reduction in absolute value is due to a reduction in the scattering density of the amorphous background is again partly true. However, the unexpected increase in scattering density of the amorphous lamellae will also contribute to the changes in the value of $\Delta\rho_u$.

To understand exactly what changes are taking place within the different regions within the granule we must consider how the water content and starch densities are affected by gelatinisation. This information is contained in Figs 6 and 7. Fig. 7 suggests that, for temperatures up to 70 °C, the molecular starch densities of all three regions remain relatively constant during gelatinisation. This finding is consistent with the work of Blanshard et al. [30], who found that gelatinisation did not lead to a major disturbance in the dimensions of the amylopectin molecule. If the dimensions are not disturbed, the density must also remain constant.

Since the amylopectin molecular density remains constant during gelatinisation, any changes in scattering density must therefore arise from variations in water content within the three regions. Fig. 6a indicates that the water content within the amorphous background region increases rapidly prior to the peak of the gelatinisation endotherm, before attaining a constant value, whereas there is a steady drop in the water content of the amorphous lamellae, from 40 °C, throughout the gelatinisation process. The water content of the crystalline lamellae drops above 40 °C, followed by an increase in water content immediately prior to and just after the peak of the DSC endotherm. These effects suggest that it is the uptake of water by the amorphous background that is of prime importance prior to the peak of the gelatinisation endotherm. However, this uptake of water not only involves the water surrounding the granules, but also water contained within the granules. In the early stages of gelatinisation, water is sucked into the rapidly swelling amorphous background region from both the amorphous and, to a lesser extent, the crystalline lamellae. At around the peak of the DSC endotherm, the rapid swelling and water uptake of the amorphous background region ceases. After this point, the crystalline packing of the double helices within the crystalline lamellae starts to be lost. As the order within the crystalline lamellae is lost, this region takes up water from the amorphous lamellae. That this is so may be a consquence of heating rate, so that kinetic factors are coming into play. It is possible that at lower heating rates, equilibrium levels of water can be drawn into the amorphous growth ring from outside the granule without perturbing the level of water in the amorphous lamellae. Further work is in progress to explore this issue, by looking both at the effect of holding granules at a fixed temperature within the endotherm and by altering the heating

rate. Such experiments should indicate how important kinetics are.

The information from this SANS study therefore supports the conclusions postulated to explain the changes in electron density measured from SAXS profiles. In excess water, gelatinisation is a two stage process. The first stage occurs immediately prior to the gelatinisation endotherm detected by DSC, when the amorphous background region starts to swell dramatically and to take up water. The second stage is reached when this dramatic swelling process causes the disruption of crystallinity within the crystalline lamellae. These results are broadly consistent with the Donovan [12,31] gelatinisation mechanism. It must be noted that this data has only to date been obtained on one species. Further work is in progress to test the generality of these observations.

However, unlike the SAXS data, the ability to measure SANS profiles with different scattering densities of absorbed water has enabled us to identify the precise changes taking place during gelatinisation within each region of the starch granule. It now appears that the water taken up by the amorphous background region does not come solely from the water surrounding the granule. Rather, as the granule swells within the amorphous background region, water is sucked out of both the amorphous lamellae and the crystalline lamellae. As gelatinisation proceeds, the swelling and water uptake of the amorphous background region reaches a maximum. As the crystallinity of the crystalline lamellae is disrupted by the swelling process, so this region takes up water. Some of this water is provided by the amorphous lamellae.

The results presented here are not fully consistent with any of the current gelatinisation mechanisms. It is therefore necessary to propose a modified gelatinisation mechanism. To summarise the findings of this paper and our earlier ones, and, gathering the results from the different starches and techniques, we find that: (i) the semicrystalline lamellae do not expand radially, as confirmed also in [29]; (ii) crystallinity is principally, but not exclusively, lost during the DSC gelatinisation endotherm; (iii) SAXS indicates that initial changes in scattering density occur within the amorphous background and/or amorphous lamellae, with changes in crystalline lamellae scattering density occurring later; (iv) SANS suggests these changes are associated with an initial rapid uptake of water by the amorphous background region. Some of this water comes from the amorphous lamellae. Later changes involve an equalisation in water contents between crystalline and amorphous lamellae.

As postulated by Donovan [12], gelatinisation is primarily a swelling-driven process. Water uptake by the amorphous background is accompanied by swelling within this region. The semicrystalline lamellar region does not expand radially. However, the amylopectin molecules at the edges of the lamellar stack will also form bonds within the amorphous regions. This couples the semicrystalline regions to the amorphous regions. As a consequence, swelling within the amorphous regions imposes a stress upon the amylopectin crystallites. This stress causes the amylopectin double helices within the crystallites to lose registry leading to the loss of crystallinity. This swelling-driven crystallite disruption process is associated with the G endotherm observed in DSC studies of starch gelatinisation in excess water. A crucial question, which ongoing experiments aim to address, is whether there is a critical level of water (and hence swelling) required in the amorphous background region for this destabilisation to occur. The answer to this question could provide at least a partial answer as to why the gelatinisation endotherm varies from species to species, as their propensity for water uptake differs.

## 5. Conclusions

By combining simultaneous SAXS/WAXS data with the results from DSC and SANS experiments, it was possible to study the nature of the gelatinisation process in more detail for a variety of starches. It was found that all starches studied here by SAXS/WAXS behaved in broadly the same way. Most of the crystallinity loss occurred during the gelatinisation endotherm, but this occurred only after a significant amount of water had already entered the amorphous background region, which has been tentatively identified with the amorphous growth ring seen in etched SEM micrographs. The amorphous background is where all the initial swelling is concentrated, and the repeat distance of the semicrystalline stack remains unchanged at all times during gelatinisation. The driving force for water uptake appears to be so strong in the amorphous background region that SANS on waxy maize shows it appears to pull

water out of the amorphous lamellae. We suggest this is because the rate of transport of water from outside the granule is not sufficiently fast on its own to accomodate the potential swelling process.

It appears that only once a large amount of swelling has occurred in the amorphous background is there sufficient stress imposed, by virtue of the connectivity of molecules from the growth ring into the semicrystalline lamellae, to start disrupting the crystals themselves. Thus the final loss of crystallinity and ultimate breakdown of the granule only occurs quite late in the gelatinisation process.

## Acknowledgements

The financial support of the BBSRC and Dalgety plc through a Cooperative studentship is acknowledged. The authors are grateful to Drs Peter Frazier and Adrian Rennie for fruitful discussions, and to Dr Richard Heenan at RAL and Dr W. Bras at Daresbury for assistance with the scattering experiments and analysis.

## References

[1] J.M.V. Blanshard, in T. Galliard (Ed.), *Starch: Properties and Potential*, Wiley, 1987, pp 17–78.
[2] R.D. Hill and B.L. Dronzek, *Stärke*, 25 (1973) 367–372.
[3] D. French, in R.L. Whistler, J.N. BeMiller, and E.F. Paschall (Eds.), *Starch: Chemistry and Technology*, 2nd ed., Academic Press, London, 1984, pp 183–247.
[4] H. Liu, J. Lelievre, and W. Ayong-Chee, *Carbohydr. Res.*, 210 (1991) 79–87.
[5] D. Cooke and M.J. Gidley, *Carbohydr. Res.*, 227 (1992) 103–112.
[6] M.J. Gidley and D. Cooke, *Biochem. Soc. Trans.*, 19 (1991) 551–555.
[7] R.E. Cameron and A.M. Donald, *Polymer*, 33 (1992) 2628–2635.
[8] R.E. Cameron and A.M. Donald, *Carbohydr. Res.*, 244 (1993) 225–236.
[9] R.E. Cameron and A.M. Donald, *J. Polym. Sci., Part B: Polym. Phys.*, 31 (1993) 1197–1204.
[10] M. Buttrose, *J. Cell Biol.*, 14 (1962) 159–167.
[11] P.J. Jenkins, R.E. Cameron, A.M. Donald, W. Bras, G.E. Derbyshire, G.R. Mant, and A.J. Ryan, *J. Polym. Sci., Part B: Polym. Phys.*, 32 (1994) 1579–1583.
[12] J. Donovan, *Biopolymers*, 18 (1979) 263–275.
[13] H.F. Zobel, S.N. Young, and L.A. Rocca, *Cereal Chem.*, 65 (1988) 443–446.
[14] I. Evans and D. Haisman, *Stärke*, 34 (1982) 224–231.
[15] C. Biliaderis, C. Page, T. MauriceB. Juliano, *J. Agric. Food Chem.*, 34 (1986) 6–14.
[16] K.J. Zeleznak and R.C. Hoseney, *Cereal Chem.*, 121 (1987) 121–124.
[17] H. Liu and J. Lelivre, *Carbohydr. Res.*, 219 (1991) 23–32.
[18] H. Liu and J. Lelivre, *Stärke*, 43 (1991) 225–227.
[19] W. Bras, G.E. Derbyshire, A.J. Ryan, G.R. Mant, F. Belton, R.A. Lewis, C.J. Hall, and G.M. Greaves, *Nucl. Instrum. Methods Phys. Res. A*, 326 (1993) 587–591.
[20] W. Bras, G.E. Derbyshire, A. Devine, S.M. Clark, J. Cooke, B.E. Komanschek, and A.J. Ryan, *J. Appl. Crystallogr.*, 28 (1995) 26–32.
[21] R. Hultgren, N.S. Gringrich, and B.E. Warren, *J. Chem. Phys.*, 3 (1935) 351–355.
[22] J.H. Wakelin, H.S. Virgil, and E. Crystal, *J. Appl. Phys.*, 30 (1959) 1654–1662.
[23] P.J. Jenkins and A.M. Donald, *Polymer*, 37 (1996) 5559–5568.
[24] P.J. Jenkins and A.M. Donald, *Int. J. Biol. Macromol.*, 17 (1995) 315–321.
[25] S. Nara, H. Takeo, and T. Komiya, *Stärke*, 33 (1981) 329–331.
[26] P.J. Jenkins, R.E. Cameron, and A.M. Donald, *Stärke*, 45 (1993) 417–420.
[27] T.A. Waigh, PhD thesis, Cambridge University, 1997.
[28] W. Leszczyñski, *Stärke*, 39 (1987) 375–378.
[29] P.J. Jenkins and A.M. Donald, *J. Appl. Polym. Sci.*, 66 (1997) 225–232.
[30] J.M.V. Blanshard, D.R. Bates, A.H. Muhr, D.L. Worcester, and J.S. Higgins, *Carbohydr. Polym.*, 4 (1984) 427–442.
[31] J. Donovan and C. Mapes, *Stärke*, 32 (1980) 190–193.
[32] G.R. Ziegler, D.B. Thompson, and J. Casasnovas, *Cereal Chem.*, 70 (1993) 247–251.